



HHS Public Access

Author manuscript

Neurochem Res. Author manuscript; available in PMC 2017 January 17.

Published in final edited form as:

Neurochem Res. 2008 July ; 33(7): 1373–1383. doi:10.1007/s11064-008-9595-y.

Chronic Carbamazepine Administration Attenuates Dopamine D₂-like Receptor-Initiated Signaling via Arachidonic Acid in Rat Brain

Mireille Basselin, Lisa Chang, Mei Chen, Jane M. Bell, and Stanley I. Rapoport

Brain Physiology and Metabolism Section, National Institute on Aging, National Institutes of Health, Bldg. 9, Room 1S126, Bethesda, MD 20892, USA

Abstract

Observations that dopaminergic antagonists are beneficial in bipolar disorder and that dopaminergic agonists can produce mania suggest that bipolar disorder involves excessive dopaminergic transmission. Thus, mood stabilizers used to treat the disease might act in part by downregulating dopaminergic transmission. In agreement, we reported that dopamine D₂-like receptor mediated signaling involving arachidonic acid (AA, 20:4n-6) was downregulated in rats chronically treated with lithium. To see whether chronic carbamazepine, another mood stabilizer, did this as well, we injected i.p. saline or the D₂-like receptor agonist, quinpirole (1 mg/kg), into unanesthetized rats that had been pretreated for 30 days with i.p. carbamazepine (25 mg/kg/day) or vehicle, and used quantitative autoradiography to measure regional brain incorporation coefficients (k*) for AA, markers of signaling. We also measured brain prostaglandin E₂ (PGE₂), an AA metabolite. In vehicle-treated rats, quinpirole compared with saline significantly increased k* for AA in 35 of 82 brain regions examined, as well as brain PGE₂ concentration. Affected regions belong to dopaminergic circuits and have high D₂-like receptor densities. Chronic carbamazepine pretreatment prevented the quinpirole-induced increments in k* and in PGE₂. These findings are consistent with the hypothesis that effective mood stabilizers generally downregulate brain AA signaling via D₂-like receptors, and that this signaling is upregulated in bipolar disorder.

Keywords

Bipolar disorder; Carbamazepine; Phospholipase A₂; D₂-like receptors; Quinpirole; Arachidonic acid; Prostaglandin E₂; Brain imaging

Introduction

Lithium, valproic acid and carbamazepine (5H-dibenz[b,f]azepine-5-carboxamide) (CBZ) are used to treat mania in bipolar disorder, but whether they have a common mechanism of action is not agreed on [3]. One possibility is that these agents correct a neurotransmission imbalance that contributes to bipolar symptoms. Clinical evidence suggests that excessive or abnormal dopaminergic signaling contributes to this neurotransmission imbalance [13, 28,

Correspondence to: Mireille Basselin.

None of the authors has a financial or other conflict of interest related to this work.

31]. Thus, drugs that inhibit dopaminergic transmission (e.g., haloperidol) have an antimanic action in bipolar disorder [20], whereas drugs that stimulate dopamine synthesis (levodopa), bind to dopamine receptors (bromocriptine), or reduce dopamine reuptake (amphetamine), often precipitate mania [1, 40].

Brain signal transduction mediated by dopaminergic D₂-like (D₂, D₃ and D₄) receptors can be coupled to the activation of Ca²⁺-dependent cytosolic phospholipase A₂ (cPLA₂), to selectively release arachidonic acid (AA, 20:4n-6), from the stereospecifically numbered (*sn*)-2 position of membrane phospholipid [53]. The signaling process can be imaged in unanesthetized rats by injecting intravenously [1-¹⁴C]AA and measuring tracer AA uptake into brain using quantitative autoradiography. Regional brain AA incorporation coefficients k* (brain radioactivity/integrated plasma radioactivity) are calculated and, if multiplied by unlabeled unesterified plasma AA concentrations, are converted to regional incorporation rates *J_{in}* that represent regional brain AA consumption. Both k* and *J_{in}* are independent of changes in cerebral blood flow [44, 46]. Increments in k* caused by drug reflect the quantity of unesterified AA released *and* then metabolized to eicosanoids (e.g. prostaglandin E₂ (PGE₂), thromboxane B₂ (TXB₂)) and other products [9, 10]. Unesterified AA as well as its eicosanoid metabolites are bioactive and can influence many physiological processes, including membrane excitability, gene transcription, apoptosis, sleep, brain blood flow and behavior [49].

Consistent with inhibition of dopaminergic receptor-mediated signaling by mood stabilizers, we reported that chronic LiCl feeding, sufficient to produce therapeutically relevant plasma and brain lithium concentrations, blocked k* signals caused by administration of the D₂-like receptor agonist, quinpirole, to unanesthetized rats [5]. In control animals fed a LiCl-free diet, quinpirole-induced increases in k* are robust and widespread in brain regions within dopaminergic circuits, and can be blocked by pre-treatment with the D₂-like receptor antagonists, butaclamol or raclopride [16, 29]. In addition to LiCl, chronic CBZ has been reported to attenuate dopamine function in rats, suggesting that normalization of a dysfunctional dopamine neurotransmission may underlie CBZ effects in bipolar disorder [2, 4, 35, 38].

In the present study, we determined if chronic CBZ administration, like chronic LiCl, would block the k* increments in response to quinpirole, and would influence brain PGE₂ or TXB₂ concentrations at rest or following drug. We measured these global brain concentrations, as well as k* for AA in 82 brain regions, in unanesthetized rats that had been treated daily for 30 days with i.p. vehicle or CBZ 25 mg/kg, then administered saline (control) or quinpirole (1.0 mg/kg i.v.). The CBZ regimen produces a plasma CBZ concentration of 54 μM, at the high end found in CBZ-treated bipolar patients (51 μM), and decreases AA turnover in brain phospholipids and the brain PGE₂ concentration [2, 11, 18, 27]. The quinpirole dose increases k* for AA significantly in brain dopaminergic circuits [5, 15].

Experimental Procedures

Animals and Diets

The study was approved by the National Institutes of Health (NIH) Animal Care and Use Committee in accordance with NIH Guidelines on the Care and Use of Laboratory Animals. Two-month-old male Fischer CDF (F-344)/CrIBR rats (Charles River Laboratories, Wilmington, MA, USA) were acclimatized for 1 week in an animal facility in which temperature, humidity and light cycle were regulated, and had ad libitum access to food (NIH-31 diet, Zeigler, Gardners, PA, USA) and water. The diet contained (as percent of total fatty acids): 20.1% saturated, 22.5% monounsaturated, 47.9% linoleic, 5.1% α -linolenic, 0.02% AA, 2.0% eicosapentaenoic, and 2.3% docosahexaenoic acid.

Drugs

[1-¹⁴C]AA in ethanol (53 mCi/mmol, >98% pure, Moravек Biochemicals, Brea, CA, USA) was evaporated and resuspended in HEPES buffer, pH 7.4, containing 50 mg/ml fatty acid-free bovine serum albumin (Sigma-Aldrich, St Louis, MO, USA). CBZ-treated rats received 25 mg/kg intraperitoneally once daily for 30 days (Sigma-Aldrich). The CBZ was dissolved in a 50:50 (v/v) dimethyl sulfoxide (DMSO, 99.9% Sigma-Aldrich): saline (0.9% NaCl, Hospira Inc., Lake Forest, IL, USA) mixture and kept at 37°C as described previously [2, 11, 27]. A control group received the same volume of DMSO:saline (vehicle) under parallel conditions. The acute 1 mg/kg i.v. dose of (-)-quinpirole hydrochloride (Sigma-Aldrich), a selective D₂-like dopamine receptor agonist [47], was chosen because it does not cause convulsions but produces widespread significant increments in k* for AA in the brain of unanesthetized rats that can be blocked by D₂-like receptor antagonists [5, 15].

Surgical Procedures and Tracer Infusion

On the morning of day 30 of chronic treatment, a rat was injected with the last CBZ or vehicle dose and then anesthetized with 2–3% halothane in O₂. Polyethylene catheters (PE 50) were inserted into the right femoral artery and vein as described previously [5]. The wound was closed with surgical clips and the rat was wrapped loosely, with its upper body remaining free, in a fast-setting plaster cast taped to a wooden block. Surgery lasted 20–25 min. The rat was allowed to recover from anesthesia for 4 h in an environment maintained at 25°C. Body temperature was maintained at 36.4–37.1°C using a feedback-heating device and rectal thermometer. Arterial blood pressure and heart rate were measured with a blood pressure recorder (CyQ 103/302; Cybersense, Inc., Nicholasville, KY, USA). Arterial blood pH, pO₂ and pCO₂ were measured with a blood gas analyzer (Model 248, Bayer Health Care, Norwood, MA, USA).

One minute after an i.v. injection of quinpirole or saline, [1-¹⁴C]AA (170 μ Ci/kg) in 2 ml was infused into the femoral vein for 5 min at a rate of 400 μ l/min, using an infusion pump (Harvard Apparatus Model 22, Natick, MA, USA). Twenty min after beginning tracer infusion, the rat was killed with an overdose of Nembutal® (100 mg/kg, i.v.) and decapitated. The brain was removed (<30 s), frozen in 2-methylbutane maintained at –40°C with dry ice, and stored at –80°C until sectioned.

Chemical Analysis

Thirteen arterial blood samples were collected before, during and after [1-¹⁴C]AA infusion, and were centrifuged immediately (30 s at 18,000g). Total lipids were extracted from 30 µl of plasma with 3 ml chloroform:methanol (2:1, by vol) and 1.5 ml 0.1 M KCl using the Folch procedure [26]. Radioactivity was determined at an efficiency of 88% in 100 µl of the lower organic phase by liquid scintillation counting. As reported, following 5 min [1-¹⁴C]AA infusion, 98% of total plasma radioactivity was radiolabeled AA [11]. Concentrations of unesterified fatty acids were determined in 100–150 µl of the frozen arterial plasma. Total lipids were extracted by the method of Folch et al. [26], and were separated by thin layer chromatography on silica gel 60 plates (Whatman, Clifton, NJ, USA) using the solvent system, heptane:diethylether:glacial acetic acid (60:40:3, by vol). Unesterified fatty acids were scraped from the plate and methylated with 1% H₂SO₄ in anhydrous methanol for 3 h at 70°C. Fatty acid methyl esters were then separated and quantified by gas chromatography using an internal standard, heptadecanoic acid (17:0) [11].

Quantitative Autoradiography

Frozen brains were cut in serial 20-µm thick coronal sections in a cryostat at –20°C. Sections were placed for 5 weeks with calibrated [¹⁴C]methylmethacrylate standards on Kodak Ektascan C/RA film (Eastman Kodak Company, Rochester, NY, USA). Brain regions from autoradiographs were identified from a stereotaxic rat brain atlas [39], and were sampled in both hemispheres. The average of bilateral measurements for each region from three consecutive brain sections was used to calculate regional radioactivity (nCi/g of brain) by digital quantitative densitometry, using a Macintosh computer and the public domain NIH Image program 1.62 (developed at the US National Institutes of Health and available on the Internet at <http://rsb.info.nih.gov/nih-image/>). Regional incorporation coefficients k^* (ml plasma/s/g brain) of AA were calculated as [46],

$$k^* = \frac{c_{brain}^*(20 \text{ min})}{\int_0^{20} c_{plasma}^* dt} \quad (1)$$

c_{plasma}^* equals plasma radioactivity determined by scintillation counting (nCi/ml), c_{brain}^* equals brain radioactivity (nCi/g of brain), and t equals time (min) after beginning of [1-¹⁴C]AA infusion.

Rates of incorporation of unesterified AA from plasma into brain phospholipids, J_{in} (fmol/s/g) were calculated as,

$$J_{in} = k^* c_{plasma} \quad (2)$$

where c_{plasma} is the plasma concentration of unlabeled unesterified AA (nmol/ml).

Brain PGE₂ and TXB₂ Concentrations

In separate experiments, on the morning of day 30, rats received the last injection of CBZ or vehicle, and 3 h and 30 min later were injected i.v. with quinpirole (1 mg/kg) or saline. Twenty-one minutes later, they were anesthetized with Nembutal® (50 mg/kg, i.p.) and subjected to high-energy head-focused microwave irradiation (5.5 kW, 3.8 s; Cober Electronics, Stamford, CT, USA) to stop post-mortem changes, such as formation of prostaglandins and fatty acid release from phospholipid [41]. Half-brains were weighed, homogenized with 18 volumes of hexane:isopropanol (3:2, by vol) using a glass Tenbroeck homogenizer and the homogenate was centrifuged for 5 min at 800g. Tissue residues were rinsed with 3 × 2 vol of the same solvent. The resultant lipid extract was concentrated to dryness under nitrogen and resuspended in the enzyme immunoassay buffer provided with a polyclonal PGE₂ or TXB₂ kit (Oxford Biochemical Research, Oxford, MI, USA).

Statistical Analyses

An unpaired two-tailed *t*-test was used to compare mean physiological parameters in CBZ- and vehicle-treated rats, using GraphPad Prism version 4.0b (GraphPad Software, San Diego, CA, www.graphpad.com). A standard two-way ANOVA, comparing CBZ administration (CBZ vs. vehicle) with drug (quinpirole vs. saline) was performed to compare arterial plasma radioactivity input functions, plasma unesterified fatty acid concentrations, brain eicosanoid concentrations and regional values of k^* and J_{in} using SPSS 11.0 (SPSS Inc., Chicago, IL, USA, <http://www.spss.com>). Where interactions between CBZ and quinpirole were statistically insignificant, probabilities of effects of CBZ and quinpirole were reported. Where interactions were statistically significant, these probabilities were not reported because they cannot be interpreted [51]. Instead, unpaired two-tailed *t*-tests were used to compare quinpirole and saline responses between CBZ- and vehicle-treated rats as well as saline responses in CBZ-compared with vehicle-treated rats. Other comparisons were not considered relevant. A post-hoc test was not used to avoid a correction for multiple comparisons. However, when a Bonferroni post-hoc test with correction for three comparisons was performed, statistical significance of differences were not changed. Data are reported as means ± SD, with statistical significance taken as $P < 0.05$.

Results

Physiology, Behavior and Arterial Plasma Radioactivity

At surgery, CBZ-treated rats had a lower mean body weight than vehicle-treated rats, 269 ± 11 g ($n = 12$) versus 281 ± 11 g ($n = 12$) ($P = 0.02$). Quinpirole (1 mg/kg) provoked behavioral cycles, each consisting of an “activity” period (repetitive sniffing, mouth and head-turning) followed by a “calm” period, whereas saline did not obviously affect behavior (Table 1). No significant difference in mean cycling periods was observed in CBZ-treated compared to vehicle-treated rats (Table 1). Compared with saline, quinpirole did not significantly affect arterial pH, pCO₂ or pO₂, or blood pressure or heart rate (Table 1).

Following intravenous [1-¹⁴C]AA infusion, neither CBZ nor quinpirole modified the integral of plasma radioactivity in the organic fraction, the input function for determining k^* in Eq. 1. The mean integral, (nCi × s)/ml ($n = 5-6$), did not differ significantly between

groups: vehicle plus saline, $213,888 \pm 28,329$; vehicle plus quinpirole, $253,791 \pm 32,823$; CBZ plus saline, $194,933 \pm 15,343$; CBZ plus quinpirole, $215,594 \pm 14,957$.

Plasma Concentrations of Unlabeled Unesterified Fatty Acids

A two-way ANOVA showed statistically insignificant interactions between CBZ and quinpirole with regard to eight of the measured plasma concentrations of unesterified fatty acids, including AA (Table 2). Chronic CBZ compared with vehicle had a negative main effect on oleic, linoleic, α -linolenic and docosahexaenoic acid concentrations (Table 2). Quinpirole did not have a main effect on any concentration.

Regional Brain AA Incorporation Coefficients, k^*

Figure 1 presents coronal autoradiographs of brains from rats treated chronically with vehicle or CBZ, then injected acutely with either saline or quinpirole. It illustrates that quinpirole increased k^* for AA in multiple brain regions in the vehicle- but not CBZ-pretreated rats. Data from such autoradiographs were collated and analyzed in Table 3.

Quinpirole Administration in Vehicle-Treated Rats

Mean AA incorporation coefficients, k^* , determined in each of 82 brain regions, were subjected to a two-way ANOVA (Table 3). Statistically significant interactions between quinpirole and CBZ were found in 30 regions. In 29 of these, t -tests showed that quinpirole compared with saline significantly increased k^* in the vehicle-treated rats. The regions, many of which belong to dopamine circuits [21], include prefrontal layer IV (18%), frontal 10 and 8 (16–36%), anterior cingulate (16%), motor (21–44%), somatosensory (21–65%), auditory (19–23%) and visual layer IV cortical areas (20%), diagonal band ventral (19%), nucleus accumbens (38%), caudate-putamen (21–31%), medial septal nuclei (28%), 2 regions of the thalamus (11–27%), and the substantia nigra (22%).

Quinpirole also significantly increased k^* for AA in 6 regions having statistically insignificant CBZ \times quinpirole interactions—lateral and medial habenular nuclei (12% and 9%, respectively), dorsal lateral geniculate nucleus (27%), ventroposterior thalamus nucleus lateral (14%), paratenial thalamus nucleus (24%), and olfactory tubercle (17%). In total, then, 35 brain regions were significantly activated by quinpirole in vehicle-treated control rats. The pattern of significant activations is illustrated in a sagittal representation of the brain in Fig. 2a.

Effects of Chronic CBZ Administration at Baseline

In the 30 regions in which CBZ \times quinpirole interactions were statistically significant, t -tests showed that chronic CBZ did not significantly change mean baseline (acute saline) k^* in any region. Where CBZ \times quinpirole interactions were statistically insignificant, chronic CBZ reduced k^* in 4 regions: visual cortex layer VI (–11%), hippocampus CA1 (–12%), lateral septal nucleus (–13%) and grey layer of the superior colliculus (–14%) (Table 3, Fig. 2b).

Effects of Quinpirole in Chronic CBZ-Treated Rats

Of the 30 regions in which CBZ \times quinpirole interactions were statistically significant, quinpirole compared with saline reduced k^* in somatosensory cortex layer II–III (–15%)

and auditory cortex layer IV (-12%) (Fig. 2c). In the 6 regions in which CBZ \times quinpirole interactions were statistically insignificant and in which quinpirole had a significant effect in vehicle-treated rats, chronic CBZ had a main effect by preventing the quinpirole-induced k^* increments (Table 3).

Regional Rates of Incorporation of Unlabeled Unesterified AA into Brain

Baseline (following saline)- and quinpirole-induced regional values of J_{in} were calculated by Eq. 2 (data not shown). Because the mean plasma concentration of unlabeled unesterified AA did not differ significantly between chronic CBZ- and vehicle-treated rats (Table 2), baseline differences and percent changes in J_{in} corresponded to the differences and percent changes in respective values of k^* (Table 3). In vehicle-treated rats, baseline values of J_{in} ranged from 4.5 fmol/s/g in the internal capsule to 36.1 fmol/s/g in the choroid plexus. In CBZ-treated rats, no baseline value of J_{in} differed significantly from its respective value in vehicle-treated rats; J_{in} ranged from 3.9 fmol/s/g in the periventricular of the hypothalamus to 30.9 fmol/s/g in the choroid plexus. As noted above, J_{in} increments following quinpirole in the vehicle-treated rats did not differ significantly from respective increments the CBZ-treated rats (data not shown).

Brain PGE₂ and TXB₂ Concentrations

A two-way ANOVA demonstrated both significant and insignificant interactions between CBZ and quinpirole with regard to brain PGE₂ and TXB₂ (Table 4). Consequent *t*-tests showed that chronic CBZ decreased the basal PGE₂ concentration by 25% ($P = 0.048$). Acute quinpirole increased brain PGE₂ by 67% ($P = 0.011$) in vehicle-treated rats, whereas chronic CBZ prevented this increase. CBZ and quinpirole had main effects on TXB₂ (Table 4). Chronic CBZ decreased the basal TXB₂ concentration by 35%. Quinpirole reduced the TXB₂ concentration by 23% in vehicle-treated rats but had no effect in the CBZ-treated rats (Table 4).

Discussion

Chronic administration of CBZ, sufficient to produce a plasma CBZ concentration therapeutically relevant to bipolar disorder, blocked the increments in k^* for AA and in whole brain PGE₂ and TXB₂ concentrations that were produced in chronic vehicle-treated rats injected with quinpirole. Chronic CBZ by itself reduced k^* in four regions as well as global brain concentrations of PGE₂ and TXB₂.

The effects in rats of chronic CBZ on baseline brain AA cascade markers, and on quinpirole-induced changes in these markers, are comparable to those produced by chronic LiCl feeding [5]. For example, chronic LiCl like chronic CBZ blocked quinpirole-induced increments in k^* for AA (we have not as yet examined lithium's ability to block the PGE₂ increment following quinpirole). Both chronic LiCl and CBZ reduced AA turnover in rat brain phospholipids, brain mRNA, protein and activity levels of cPLA₂, and the DNA-binding capacity and protein level of a cPLA₂ transcription factor, activator protein-2 [11, 19, 27, 42, 43, 45]. These observations, plus clinical data that dopaminergic neurotransmission is disturbed in bipolar disorder [13, 28, 31], and that dopamine receptor

antagonists can be therapeutic whereas drugs that stimulate dopamine synthesis, bind to dopamine receptors or reduce dopamine reuptake often precipitate mania (see “Introduction”), suggest that mood stabilizers are therapeutic in bipolar disorder in part by suppressing excessive D₂-like receptor signaling involving AA.

CBZ could have downregulated the D₂-like receptor-initiated AA signal by reducing synaptic dopamine release and synthesis, D₂ receptor density, D₂-like coupled G $\alpha_{o/i}$, D₂-like receptor phosphorylation, or histone deacetylation by histone deacetylase [2, 14, 32, 34, 35, 38]. CBZ also could have altered G-protein receptor kinase translocation from cytosol to cell membrane, and thus densitization of D₂-like receptors [24]. CBZ’s ability to reduce rat brain cPLA₂ transcription and COX activity also could have contributed to the reduced signaling, associated with reduced basal PGE₂ and TXB₂ concentrations and reduced quinpirole-induced changes in these concentrations [8, 27]. PGE₂ and TXB₂ are converted preferentially from AA by COX-2 and COX-1, respectively. When these enzymes are pharmacologically inhibited or knocked out in rodent models, k* responses to drugs acting at cPLA₂-coupled neuroreceptors are reduced or lost, as are the increments in brain PGE₂ and/or TXB₂ concentrations [9, 10]. Our finding that quinpirole elevated brain PGE₂ in vehicle-treated rats agrees with prior in vitro and in vivo observations [23]. The mechanism for the reduction of brain TXB₂ by quinpirole is not apparent but might be elucidated by studying the drug effect on COX-1 and thromboxane synthase expression in brain.

The baseline values of k* for AA in vehicle-treated rats, which ranged from 2.65 to 20.9 $\times 10^{-4}$ ml/s/g brain, are similar to previously reported values [5, 6, 8, 10, 15]. Quinpirole significantly increased k* in 35 regions, many of which belong to dopaminergic circuits containing D₂ receptors (e.g. caudate-putamen and substantia nigra) [33], D₃ receptors (e.g. nucleus accumbens and olfactory tubercle) [50] or D₄ receptors (e.g. cerebral cortex) [55]. Giving selective D₂, D₃ and D₄ agonists or antagonists might identify the contributions of the different receptor subtypes to the k* signal. Furthermore, regional baseline values of J_{in} in vehicle-treated rats, 4.5–36.1 fmol/s/g, agree with a published global value of 6.57 fmol/s/g [11]. Given that J_{in} represents the regional rate of metabolic AA loss from brain [10, 44], our data on J_{in} indicate comparable baseline rates of AA loss in vehicle- and CBZ-treated rats.

Chronic CBZ, unlike chronic lithium [5, 12] did not prevent the quinpirole induced hyperactivity or stereotypy (Table 1). Chronic CBZ or chronic valproate also do not affect quinpirole-induced locomotor activity [48]. As each of the three anti-bipolar agents downregulates the brain AA cascade, their different effects on quinpirole-induced behaviors suggest that these behaviors don’t involve AA signaling and, moreover, that the quinpirole-induced activity cycles are not modeling bipolar disorder [48].

In addition to attenuating D₂-like receptor-mediated AA signaling, chronic lithium, CBZ and valproic acid [6–8] each attenuates AA signaling mediated by glutamatergic N-methyl-D-aspartate (NMDA) receptors in unanesthetized rats [6, 8]. As D₂-like and NMDA receptors are often functionally coupled and co-localized on the same neurons in brain [52, 54], these data suggest that mood stabilizers that are effective against mania suppress AA signaling coupled to both D₂-like and NMDA receptors. In this regard lamotrigine, which is preferred

for treating bipolar depression and rapid recycling, is considered to act in part by reducing presynaptic glutamate release [22]. A role for both receptor subtypes is consistent with evidence of disturbed dopaminergic and NMDA transmission in bipolar disorder [1, 13, 20, 28, 31, 36, 37, 40].

It now is possible to measure k^* for AA in the human brain with positron emission tomography following the intravenous injection of $[1-^{11}\text{C}]$ AA [25]. Thus, it would be of interest to see if our findings in rats can be extrapolated to bipolar disorder patients off and on treatment with mood stabilizers, by giving them dopamine receptor agonists to stimulate the AA signal, such as apomorphine or ropinerole [17, 30, 56].

In conclusion, chronic CBZ blocked the increments in k^* for AA as well in the global brain PGE_2 concentration seen in response to quinpirole in chronic-vehicle treated rats. Those and related observations regarding chronic lithium and valproic acid support the hypothesis that mood stabilizers of proven efficacy against bipolar disorder may act by downregulating brain AA signaling coupled to both D_2 -like and NMDA receptors.

Acknowledgments

This work was supported by the Intramural Research Program of the National Institute on Aging, National Institutes of Health.

Abbreviations

AA	Arachidonic acid
PLA₂	Phospholipase A ₂
cPLA₂	Cytosolic PLA ₂
sn	Stereospecifically numbered
NMDA	N-methyl-D-aspartate
CBZ	Carbamazepine
PGE₂	Prostaglandin E ₂
TXB₂	Thromboxane B ₂
COX	Cyclooxygenase

References

1. Anand A, Verhoeff P, Seneca N, et al. Brain SPECT imaging of amphetamine-induced dopamine release in euthymic bipolar disorder patients. *Am J Psychiatry*. 2000; 157:1108–1114. [PubMed: 10873919]
2. Baf MH, Subhash MN, Lakshmana KM, et al. Alterations in monoamine levels in discrete regions of rat brain after chronic administration of carbamazepine. *Neurochem Res*. 1994; 19:1139–1143. [PubMed: 7824066]

3. Barchas, J.; Hamblin, M.; Malenka, R. Biochemical hypotheses of mood and anxiety disorders. In: Siegel, GJ.; Agranoff, BW.; Albers, RW.; Molinoff, PB., editors. Basic neurochemistry. 5th. Raven Press; New York: 1994. p. 979-1001.
4. Barros HM, Leite JR. Effects of acute and chronic carbamazepine administration on apomorphine-elicited stereotypy. *Eur J Pharmacol.* 1986; 123:345–349. [PubMed: 3720822]
5. Basselin M, Chang L, Bell JM, et al. Chronic lithium chloride administration to unanesthetized rats attenuates brain dopamine D₂-like receptor-initiated signaling via arachidonic acid. *Neuropsychopharmacology.* 2005; 30:1064–1075. [PubMed: 15812572]
6. Basselin M, Chang L, Bell JM, et al. Chronic lithium chloride administration attenuates brain NMDA receptor-initiated signaling via arachidonic acid in unanesthetized rats. *Neuropsychopharmacology.* 2006; 31:1659–1674. [PubMed: 16292331]
7. Basselin M, Chang L, Chen M, et al. Chronic valproic acid reduces NMDA receptor-initiated signaling via arachidonic acid in rat brain (Abstract). *J Neurochem.* 2007; 102(Suppl 1):146.
8. Basselin M, Villacreses NE, Chen M, et al. Chronic carbamazepine administration reduces NMDA receptor-initiated signaling via arachidonic acid in rat brain. *Biol Psychiatry.* 2007; 62:934–943. [PubMed: 17628508]
9. Basselin M, Villacreses NE, Langenbach R, et al. Resting and arecoline-stimulated brain metabolism and signaling involving arachidonic acid are altered in the cyclooxygenase-2 knockout mouse. *J Neurochem.* 2006; 96:669–679. [PubMed: 16405503]
10. Basselin M, Villacreses NE, Lee HJ, et al. Flurbiprofen, a cyclooxygenase inhibitor, reduces the brain arachidonic acid signal in response to the cholinergic muscarinic agonist, arecoline, in awake rats. *Neurochem Res.* 2007; 32:1857–1867. [PubMed: 17562170]
11. Bazinet RP, Rao JS, Chang L, et al. Chronic carbamazepine decreases the incorporation rate and turnover of arachidonic acid but not docosahexaenoic acid in brain phospholipids of the unanesthetized rat: relevance to bipolar disorder. *Biol Psychiatry.* 2006; 59:401–407. [PubMed: 16182257]
12. Beaulieu JM, Sotnikova TD, Yao WD, et al. Lithium antagonizes dopamine-dependent behaviors mediated by an AKT/glycogen synthase kinase 3 signaling cascade. *Proc Natl Acad Sci USA.* 2004; 101:5099–5104. [PubMed: 15044694]
13. Berk M, Dodd S, Kauer-Sant'anna M, et al. Dopamine dysregulation syndrome: implications for a dopamine hypothesis of bipolar disorder. *Acta Psychiatr Scand.* 2007; (Suppl):41–49.
14. Beutler AS, Li S, Nicol R, et al. Carbamazepine is an inhibitor of histone deacetylases. *Life Sci.* 2005; 76:3107–3115. [PubMed: 15850602]
15. Bhattacharjee AK, Chang L, Lee HJ, et al. D₂ but not D₁ dopamine receptor stimulation augments brain signaling involving arachidonic acid in unanesthetized rats. *Psychopharmacology (Berl).* 2005; 180:735–742. [PubMed: 16163535]
16. Bhattacharjee AK, Chang L, White L, et al. D-amphetamine stimulates D₂ dopamine receptor-mediated brain signaling involving arachidonic acid in unanesthetized rats. *J Cereb Blood Flow Metab.* 2006; 26:1378–1388. [PubMed: 16511499]
17. Bhattacharjee AK, Chang L, White L, et al. Imaging apomorphine stimulation of brain arachidonic acid signaling via D₂-like receptors in unanesthetized rats. *Psychopharmacology.*
18. Bialer M, Levy RH, Perucca E. Does carbamazepine have a narrow therapeutic plasma concentration range? *Ther Drug Monit.* 1998; 20:56–59. [PubMed: 9485555]
19. Chang MC, Grange E, Rabin O, et al. Lithium decreases turnover of arachidonate in several brain phospholipids. *Neurosci Lett.* 1996; 220:171–174. *Erratum in: Neurosci Lett* 1997 31:222:141. [PubMed: 8994220]
20. Cipriani A, Rendell JM, Geddes JR. Haloperidol alone or in combination for acute mania. *Cochrane Database Syst Rev.* 2006; 3:CD004362.
21. Cooper, JR.; Bloom, FE.; Roth, RH. The biochemical basis of neuropharmacology. 8th. Oxford University Press; Oxford: 2003.
22. Cunningham MO, Jones RS. The anticonvulsant, lamotrigine decreases spontaneous glutamate release but increases spontaneous GABA release in the rat entorhinal cortex in vitro. *Neuropharmacology.* 2000; 39:2139–2146. [PubMed: 10963757]

23. Di Marzo V, Piomelli D. Participation of prostaglandin E₂ in dopamine D₂ receptor-dependent potentiation of arachidonic acid release. *J Neurochem.* 1992; 59:379–382. [PubMed: 1351931]
24. Ertley RN, Bazinet RP, Lee HJ, et al. Chronic treatment with mood stabilizers increases membrane GRK3 in rat frontal cortex. *Biol Psychiatry.* 2007; 61:246–249. [PubMed: 16697355]
25. Esposito G, Giovacchini G, Der M, et al. Imaging signal transduction via arachidonic acid in the human brain during visual stimulation, by means of positron emission tomography. *Neuroimage.* 2006; 34:1342–1351. [PubMed: 17196833]
26. Folch J, Lees M, Sloane Stanley GH. A simple method for the isolation and purification of total lipides from animal tissues. *J Biol Chem.* 1957; 226:497–509. [PubMed: 13428781]
27. Ghelardoni S, Tomita YA, Bell JM, et al. Chronic carbamazepine selectively downregulates cytosolic phospholipase A₂ expression and cyclooxygenase activity in rat brain. *Biol Psychiatry.* 2004; 56:248–254. [PubMed: 15312812]
28. Greenwood TA, Schork NJ, Eskin E, et al. Identification of additional variants within the human dopamine transporter gene provides further evidence for an association with bipolar disorder in two independent samples. *Mol Psychiatry.* 2006; 11:125–133, 115. [PubMed: 16261167]
29. Hayakawa T, Chang MC, Rapoport SI, et al. Selective dopamine receptor stimulation differentially affects [³H]arachidonic acid incorporation, a surrogate marker for phospholipase A₂-mediated neurotransmitter signal transduction, in a rodent model of Parkinson's disease. *J Pharmacol Exp Ther.* 2001; 296:1074–1084. [PubMed: 11181943]
30. Hosey LA, Thompson JL, Metman LV, et al. Temporal dynamics of cortical and subcortical responses to apomorphine in Parkinson disease: an H2150 PET study. *Clin Neuropharmacol.* 2005; 28:18–27. [PubMed: 15711435]
31. Ishikawa M, Mizukami K, Iwakiri M, et al. Immunohistochemical and immunoblot analysis of dopamine and cyclic AMP-regulated phosphoprotein, relative molecular mass 32,000 (DARPP-32) in the prefrontal cortex of subjects with schizophrenia and bipolar disorder. *Prog Neuropsychopharmacol Biol Psychiatry.* 2007; 31:1177–1181. [PubMed: 17521792]
32. Jensen JB, Mork A. Altered protein phosphorylation in the rat brain following chronic lithium and carbamazepine treatments. *Eur Neuropsychopharmacol.* 1997; 7:173–179. [PubMed: 9213075]
33. Khan ZU, Gutierrez A, Martin R, et al. Differential regional and cellular distribution of dopamine D₂-like receptors: an immunocytochemical study of subtype-specific antibodies in rat and human brain. *J Comp Neurol.* 1998; 402:353–371. [PubMed: 9853904]
34. Kim KM, Valenzano KJ, Robinson SR, et al. Differential regulation of the dopamine D₂ and D₃ receptors by G protein-coupled receptor kinases and beta-arrestins. *J Biol Chem.* 2001; 276:37409–37414. [PubMed: 11473130]
35. Lesch KP, Aulakh CS, Tolliver TJ, et al. Differential effects of long-term lithium and carbamazepine administration on G_s alpha and G_i alpha protein in rat brain. *Eur J Pharmacol.* 1991; 207:355–359. [PubMed: 1783003]
36. Martucci L, Wong AH, De Luca V, et al. N-methyl-d-aspartate receptor NR2B subunit gene GRIN2B in schizophrenia and bipolar disorder: polymorphisms and mRNA levels. *Schizophr Res.* 2006; 84:214–221. [PubMed: 16549338]
37. McCullumsmith RE, Kristiansen LV, Beneyto M, et al. Decreased NR1, NR2A, and SAP102 transcript expression in the hippocampus in bipolar disorder. *Brain Res.* 2007; 1127:108–118. [PubMed: 17113057]
38. Montezinho LP, Castro MM, Duarte CB, et al. The interaction between dopamine D₂-like and beta-adrenergic receptors in the prefrontal cortex is altered by mood-stabilizing agents. *J Neurochem.* 2006; 96:1336–1348. [PubMed: 16478526]
39. Paxinos, G.; Watson, C. *The rat brain in stereotaxic coordinates.* Academic Press; New York: 1987.
40. Peet M, Peters S. Drug-induced mania. *Drug Saf.* 1995; 12:146–153. [PubMed: 7766338]
41. Poddubiuk ZM, Blumberg JB, Kopin IJ. Brain prostaglandin content in rats sacrificed by decapitation vs focused microwave irradiation. *Experientia.* 1982; 38:987–988. [PubMed: 7128744]
42. Rao JS, Bazinet RP, Rapoport SI, et al. Chronic administration of carbamazepine downregulates AP-2 DNA binding activity and AP-2 α protein expression in rat frontal cortex. *Biol Psychiatry.* 2007; 61:154–161. [PubMed: 16806101]

43. Rao JS, Rapoport SI, Bosetti F. Decrease in the AP-2 DNA-binding activity and in the protein expression of AP-2 α and AP-2 β in frontal cortex of rats treated with lithium for 6 weeks. *Neuropsychopharmacology*. 2005; 30:2006–2013. [PubMed: 15827566]
44. Rapoport SI. In vivo approaches to quantifying and imaging brain arachidonic and docosahexaenoic acid metabolism. *J Pediatr*. 2003; 143:S26–S34. [PubMed: 14597911]
45. Rintala J, Seemann R, Chandrasekaran K, et al. 85 kDa cytosolic phospholipase A₂ is a target for chronic lithium in rat brain. *Neuroreport*. 1999; 10:3887–3890. [PubMed: 10716228]
46. Robinson PJ, Noronha J, DeGeorge JJ, et al. A quantitative method for measuring regional in vivo fatty-acid incorporation into and turnover within brain phospholipids: review and critical analysis. *Brain Res Brain Res Rev*. 1992; 17:187–214. [PubMed: 1467810]
47. Seeman P, Van Tol HH. Dopamine receptor pharmacology. *Trends Pharmacol Sci*. 1994; 15:264–270. [PubMed: 7940991]
48. Shaldubina A, Einat H, Szechtman H, et al. Preliminary evaluation of oral anticonvulsant treatment in the quinpirole model of bipolar disorder. *J Neural Transm*. 2002; 109:433–440. [PubMed: 11956963]
49. Shimizu T, Wolfe LS. Arachidonic acid cascade and signal transduction. *J Neurochem*. 1990; 55:1–15. [PubMed: 2113081]
50. Sokoloff P, Giros B, Martres MP, et al. Molecular cloning and characterization of a novel dopamine receptor D₃ as a target for neuroleptics. *Nature*. 1990; 347:146–151. [PubMed: 1975644]
51. Tabachnick, BG.; Fidell, LS. Computer-assisted research design and analysis. Allyn; Bacon, editors. Boston: 2001.
52. Tarazi FI, Baldessarini RJ. Regional localization of dopamine and ionotropic glutamate receptor subtypes in striatolimbic brain regions. *J Neurosci Res*. 1999; 55:401–410. [PubMed: 10723051]
53. Vial D, Piomelli D. Dopamine D₂ receptors potentiate arachidonate release via activation of cytosolic, arachidonic-specific phospholipase A₂. *J Neurochem*. 1995; 64:2765–2772. [PubMed: 7760057]
54. Wang X, Zhong P, Gu Z, et al. Regulation of NMDA receptors by dopamine D₄ signaling in prefrontal cortex. *J Neurosci*. 2003; 23:9852–9861. [PubMed: 14586014]
55. Wedzony K, Chocyk A, Mackowiak M, et al. Cortical localization of dopamine D₄ receptors in the rat brain—immunocytochemical study. *J Physiol Pharmacol*. 2000; 51:205–221. [PubMed: 10898094]
56. Whone AL, Watts RL, Stoessl AJ, et al. Slower progression of Parkinson's disease with ropinirole versus levodopa: the REAL-PET study. *Ann Neurol*. 2003; 54:93–101. [PubMed: 12838524]

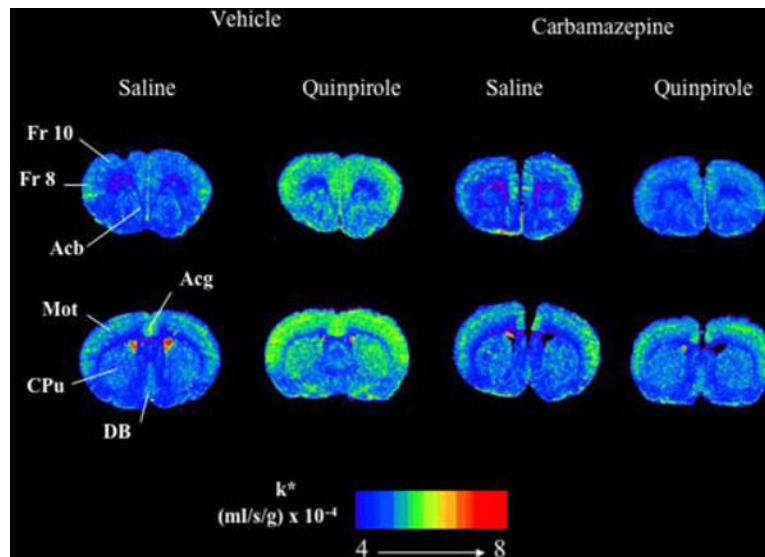


Fig. 1. Coronal autoradiographs of brains showing effects of quinpirole and carbamazepine on regional AA incorporation coefficients k^* in rats. Values of k^* ($\text{ml/s/g brain} \times 10^{-4}$) are given on a color scale from 4 (blue) to 8 (yellow-orange). Abbreviations: Acb, nucleus accumbens; Acp, anterior cingulate cortex; CPu, caudate-putamen; DB, diagonal band; Fr 8, frontal cortex area 8; Fr 10, frontal cortex area 10; Mot, motor cortex. *Note:* For interpretation of the references to color in this figure legend, the reader is referred to the online version of this article

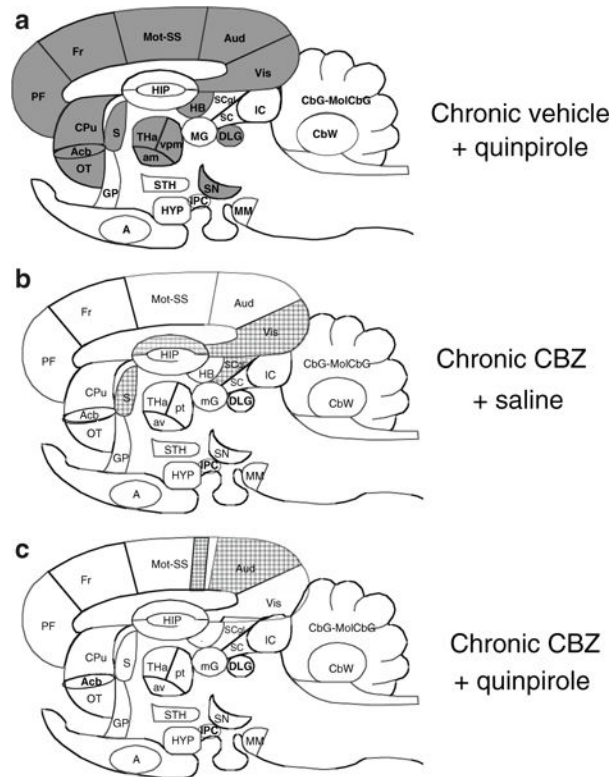


Fig. 2.

Difference patterns of k^* responses to quinpirole and carbamazepine in sagittal representation of rat brain. Regions in which k^* was increased significantly ($P < 0.05$) compared with chronic vehicle + saline are solid black, regions in which k^* was decreased significantly are hatched. List of regions: A, amygdala; Acb, nucleus accumbens; Aud, auditory cortex; av, anteroventral thalamic nucleus; CbG, cerebellar gray matter; CbW, cerebellar white matter; CPu, caudate putamen; DLG, dorsal lateral geniculate nucleus; Fr, frontal cortex; GP, globus pallidus; HB, habenular nuclei; HIP, hippocampus; HYP, hypothalamus; IC, inferior colliculus; IPC, interpeduncular nucleus; MM, mammillary nucleus; mG, medial geniculate nucleus; MolCbG, molecular layer of cerebellar gray matter; Mot, motor cortex; OT, olfactory tubercle; PF, prefrontal cortex; pt, paratenial thalamic nucleus; SN, substantia nigra; S, septum; SS, somatosensory cortex; SC, superior colliculus; SCgl, gray layer of superior colliculus; STH, subthalamic nucleus; THa, thalamus; Vis, visual cortex

Table 1

Effects of carbamazepine and quinpirole on physiological parameters

	Vehicle				Carbamazepine			
	Saline		Quinpirole		Saline		Quinpirole	
	Before	After	Before	After	Before	After	Before	After
Body temperature (°C)	36.5 ± 0.2	36.1 ± 0.2	36.4 ± 0.3	36.6 ± 0.3	36.5 ± 0.2	36.8 ± 0.4	36.5 ± 0.5	36.7 ± 0.2
Heart rate (beats/min)	384 ± 40	410 ± 34	441 ± 21	442 ± 31	417 ± 30	423 ± 23	421 ± 18	427 ± 18
Arterial blood pressure (mm Hg)								
Systolic	149 ± 7	152 ± 6	160 ± 7	154 ± 13	142 ± 13	144 ± 11	142 ± 6	149 ± 12
Diastolic	94 ± 12	92 ± 8	103 ± 9	95 ± 12	99 ± 5	97 ± 7	105 ± 5	102 ± 7
pH	7.461 ± 0.024	7.435 ± 0.012	7.465 ± 0.021	7.451 ± 0.024	7.447 ± 0.021	7.368 ± 0.182	7.462 ± 0.012	7.441 ± 0.012
pO ₂ (mm Hg)	94.7 ± 12.5	97.2 ± 4.7	97.1 ± 10.0	108 ± 18.0	94.4 ± 6.8	98.5 ± 3.9	99.6 ± 5.0	103.2 ± 3.8
pCO ₂ (mm Hg)	37.4 ± 3.6	42.4 ± 2.2	37.2 ± 3.1	35.5 ± 6.3	39.1 ± 2.6	42.4 ± 3.2	37.2 ± 2.0	39.9 ± 1.8
Orofacial activity duration (s)								
Orofacial activity				15 ± 4				14 ± 3
Calm period				34 ± 5				36 ± 4

Values are means ± SD (*n* = 6) measured before and 11 min after saline or quinpirole (1 mg/kg, i.v.) injection. None of these physiological parameters was statistically significantly affected by chronic carbamazepine or quinpirole administration

Table 2
Effects of quinpirole and carbamazepine on plasma concentrations of unlabeled unesterified fatty acid in rats

Fatty acid	Vehicle		CBZ		CBZ × quinpirole interaction <i>P</i> -value	Quinpirole effect <i>P</i> -value
	Saline (<i>n</i> = 5)	Quinpirole (<i>n</i> = 6)	Saline (<i>n</i> = 6)	Quinpirole (<i>n</i> = 6)		
<i>Concentration, nmol/ml plasma</i>						
Palmitic (16:0)	213.1 ± 47.2	247.4 ± 101.4	219.3 ± 81.1	142.2 ± 33.3	0.080	0.117
Palmitoleic (16:1 n-7)	20.5 ± 5.5	26.5 ± 11.7	19.2 ± 10.4	14.9 ± 7.6	0.202	0.115
Stearic (18:0)	37.8 ± 6.9	37.7 ± 10.5	40.5 ± 5.9	35.9 ± 2.6	0.456	0.430
Oleic (18:1 n-9)	104.9 ± 24.0	117.3 ± 52.0	90.7 ± 18.7	71.1 ± 21.0	0.250	0.790
Linoleic (18:2 n-6)	225.9 ± 52.3	277.9 ± 110.7	158.4 ± 36.6	125.2 ± 34.9	0.144	0.740
α-Linolenic (18:3 n-3)	14.1 ± 3.4	18.8 ± 7.9	8.0 ± 2.3	7.1 ± 3.3	0.183	0.354
Arachidonic (20:4 n-6)	17.2 ± 3.3	22.1 ± 9.1	16.2 ± 3.4	14.4 ± 2.1	0.150	0.497
Docosahexaenoic (22:6 n-3)	36.2 ± 5.5	33.0 ± 15.4	21.8 ± 8.1	17.9 ± 2.7	0.931	0.375

Values are mean ± SD measured from arterial plasma collected at 19 min after the beginning of [¹⁻¹⁴C]AA infusion

Table 3
Effect of chronic carbamazepine on quinpirole-induced regional AA incorporation coefficients, k* in rat brain

Brain region	Vehicle		Carbamazepine (CBZ)		CBZ × Quinpirole Interaction P-value	CBZ Effect P-value	CBZ Effect P-value
	Saline (n = 5)	Quinpirole (n = 6)	Saline (n = 6)	Quinpirole (n = 6)			
Prefrontal cortex layer I	5.03 ± 0.75	5.36 ± 0.66	5.12 ± 0.36	5.38 ± 0.25	0.302	0.523	0.745
Prefrontal cortex layer IV	5.42 ± 0.77	6.42 ± 0.62*	5.48 ± 0.52	5.86 ± 0.52	0.005		
Primary olfactory cortex	4.50 ± 0.31	5.24 ± 0.82	4.33 ± 0.61	4.40 ± 0.35	0.020		
Frontal cortex (10)							
Layer I	4.86 ± 0.28	5.66 ± 0.40**	4.20 ± 0.63	3.62 ± 0.36	0.002		
Layer IV	5.34 ± 0.50	6.68 ± 0.67**	4.71 ± 0.69	3.99 ± 0.54	0.001		
Frontal cortex (8)							
Layer I	5.00 ± 0.28	6.15 ± 0.50**	4.35 ± 0.55	3.99 ± 0.54	0.001		
Layer IV	5.52 ± 0.66	7.52 ± 0.76**	4.76 ± 0.50	4.36 ± 0.70	<0.001		
Pyriiform cortex	4.50 ± 0.55	4.30 ± 0.76	4.13 ± 0.15	4.10 ± 0.32	0.697	0.584	0.688
Anterior cingulate cortex	5.83 ± 0.76	6.79 ± 0.41**	5.32 ± 0.51	5.46 ± 0.53	0.003		
Motor cortex							
Layer I	5.09 ± 0.56	6.18 ± 0.67*	5.26 ± 0.29	5.12 ± 0.33	0.007		
Layer II–III	4.71 ± 0.21	6.26 ± 0.78**	4.30 ± 0.37	4.93 ± 0.32	<0.001		
Layer IV	5.18 ± 0.45	7.45 ± 1.16**	4.35 ± 0.42	4.71 ± 0.31	0.001		
Layer V	4.30 ± 0.32	5.34 ± 0.78*	3.97 ± 0.36	3.66 ± 0.65	0.011		
Layer VI	4.02 ± 0.21	5.43 ± 0.61***	3.72 ± 0.59	3.28 ± 0.23	<0.001		
Somatosensory cortex							
Layer I	5.10 ± 0.49	6.18 ± 0.96*	4.81 ± 0.44	4.31 ± 0.63	0.048		
Layer II–III	5.60 ± 0.77	7.36 ± 0.89**	4.93 ± 0.68	4.19 ± 0.34*	0.001		
Layer IV	5.72 ± 0.85	9.41 ± 1.33***	4.83 ± 0.47	4.30 ± 0.60	<0.001		
Layer V	5.16 ± 0.38	7.28 ± 0.85***	4.63 ± 0.56	4.02 ± 0.52	<0.001		
Layer VI	4.71 ± 0.23	7.32 ± 0.73***	4.13 ± 0.42	3.77 ± 0.42	<0.001		
Auditory cortex							

Brain region	Vehicle		Carbamazepine (CBZ)		CBZ × Quinpirole Interaction P-value	CBZ Effect P-value	CBZ Effect P-value
	Saline (n = 5)	Quinpirole (n = 6)	Saline (n = 6)	Quinpirole (n = 6)			
Layer I	5.54 ± 0.51	6.59 ± 0.69*	4.97 ± 0.41	4.74 ± 0.38	0.037		
Layer IV	6.21 ± 0.45	7.62 ± 1.12*	5.59 ± 0.55	4.91 ± 0.36*	<0.001		
Layer VI	5.43 ± 0.28	6.02 ± 0.90	4.92 ± 0.45	4.46 ± 0.36	0.037		
Visual cortex							
Layer I	5.25 ± 0.30	5.51 ± 0.67	4.81 ± 0.37	4.69 ± 0.27	0.302	0.003	0.703
Layer IV	5.64 ± 0.50	6.74 ± 0.85*	4.99 ± 0.47	4.55 ± 0.35	0.003		
Layer VI	5.32 ± 0.24	5.55 ± 0.68	4.74 ± 0.48	4.76 ± 0.55	0.799	0.021	0.427
Preoptic area (LPO/MPO)	4.33 ± 0.24	4.56 ± 0.68	4.65 ± 0.42	4.76 ± 0.55	0.801	0.512	0.478
Suprachiasmatic nu	4.94 ± 0.35	4.34 ± 0.66	4.30 ± 0.52	4.29 ± 0.56	0.217	0.148	0.195
Globus pallidus	3.94 ± 0.99	4.62 ± 0.45	3.88 ± 0.29	4.16 ± 0.57	0.442	0.307	0.074
Bed nu stria terminalis	4.34 ± 0.44	4.60 ± 0.41	4.11 ± 0.48	4.29 ± 0.45	0.319	0.054	0.064
Olfactory tubercle	4.52 ± 0.32	5.28 ± 0.52	4.26 ± 0.42	4.31 ± 0.47	0.072	0.004	0.044
Diagonal band dorsal	4.66 ± 0.21	5.39 ± 0.84	4.56 ± 0.48	4.01 ± 0.38	0.011		
Ventral	4.54 ± 0.22	5.40 ± 0.67*	4.14 ± 0.45	4.09 ± 0.52	0.042		
Amygdala basolateral/medial	5.18 ± 0.33	4.82 ± 0.65	4.64 ± 0.48	4.55 ± 0.29	0.490	0.052	0.262
Hippocampus							
CA1	4.29 ± 0.38	4.20 ± 0.58	3.77 ± 0.31	3.76 ± 0.39	0.835	0.014	0.773
CA2	4.22 ± 0.41	4.57 ± 0.65	4.05 ± 0.45	4.19 ± 0.60	0.666	0.244	0.290
CA3	4.32 ± 0.35	4.41 ± 0.49	4.03 ± 0.28	4.15 ± 0.49	0.745	0.301	0.456
Dentate gyrus	4.62 ± 0.27	5.21 ± 0.95	4.45 ± 0.25	4.50 ± 0.38	0.588	0.245	0.055
SLM	5.89 ± 0.70	5.76 ± 1.06	5.24 ± 0.28	5.28 ± 0.61	0.773	0.077	0.884
Accumbens nucleus	4.92 ± 0.24	6.79 ± 0.89**	4.66 ± 0.38	4.18 ± 0.28	0.001		
Caudate putamen							
Dorsal	4.66 ± 0.30	5.63 ± 0.57**	4.24 ± 0.42	4.16 ± 0.30	0.007		
Ventral	4.81 ± 0.26	5.89 ± 0.59**	4.44 ± 0.35	4.31 ± 0.35	0.002		
Lateral	4.72 ± 0.32	6.20 ± 0.70**	4.29 ± 0.40	4.14 ± 0.25	<0.001		
Medial	4.83 ± 0.37	6.19 ± 0.54**	4.27 ± 0.38	4.16 ± 0.26	<0.001		
Septal nu lateral	4.68 ± 0.48	4.37 ± 0.57	4.05 ± 0.34	4.10 ± 0.48	0.360	0.034	0.496

Brain region	Vehicle		Carbamazepine (CBZ)		CBZ × Quinpirole Interaction P-value	CBZ Effect P-value	CBZ Effect P-value
	Saline (n = 5)	Quinpirole (n = 6)	Saline (n = 6)	Quinpirole (n = 6)			
Septal nu medial	5.02 ± 0.35	6.42 ± 0.60**	4.65 ± 0.31	4.40 ± 0.25	<0.001		
Habenular nu lateral	6.61 ± 0.40	7.39 ± 0.56	6.23 ± 0.22	6.34 ± 0.50	0.089	0.001	0.026
Habenular nu medial	6.96 ± 0.26	7.59 ± 0.61	6.48 ± 0.37	6.78 ± 0.93	0.469	0.010	0.050
Lateral geniculate nu dorsal	5.83 ± 0.26	7.39 ± 1.48	5.32 ± 0.29	5.58 ± 0.52	0.075	0.003	0.017
Medial geniculate nu	6.27 ± 0.51	6.28 ± 0.89	6.57 ± 0.31	6.65 ± 0.23	0.883	0.745	0.836
Thalamus							
Ventroposterior lateral nu	4.77 ± 0.42	5.44 ± 0.23	4.60 ± 0.44	4.37 ± 0.32	0.175	0.001	0.009
Ventroposterior medial nu	5.56 ± 0.24	6.16 ± 0.41*	5.27 ± 0.42	5.31 ± 0.29	0.041		
Paratentorial nu	4.81 ± 0.55	5.98 ± 1.09	4.23 ± 0.37	4.27 ± 0.29	0.055	0.001	0.042
Anteroventral nu	7.39 ± 1.17	8.44 ± 1.11	6.87 ± 0.85	6.95 ± 0.67	0.381	0.236	0.301
Anteromedial nu	4.83 ± 0.21	6.14 ± 0.89*	4.39 ± 0.51	4.14 ± 0.65	0.008		
Reticular nu	5.29 ± 0.69	5.45 ± 1.10	5.28 ± 0.31	5.64 ± 0.75	0.766	0.311	0.432
Paraventricular nu	4.54 ± 0.91	4.35 ± 0.77	3.94 ± 0.47	3.83 ± 0.56	0.107	0.546	0.216
Parafascicular nu	3.83 ± 0.59	4.10 ± 0.45	4.22 ± 0.86	4.12 ± 0.59	0.506	0.467	0.753
Subthalamic nu	5.70 ± 1.43	5.26 ± 0.58	5.58 ± 0.52	5.85 ± 0.38	0.232	0.453	0.914
Hypothalamus							
Supraoptic nu	4.11 ± 0.62	4.09 ± 0.60	3.51 ± 0.33	3.97 ± 0.57	0.299	0.421	0.338
Lateral	3.67 ± 0.56	3.78 ± 0.61	3.42 ± 0.24	3.10 ± 0.42	0.299	0.325	0.609
Anterior	3.63 ± 0.74	3.25 ± 0.26	3.42 ± 0.19	2.95 ± 0.53	0.835	0.523	0.589
Periventricular	2.59 ± 0.48	2.99 ± 0.42	2.79 ± 0.14	2.49 ± 0.38	0.758	0.458	0.562
Arcuate	3.00 ± 0.51	3.42 ± 0.38	3.44 ± 0.32	3.83 ± 0.32	0.914	0.658	0.745
Ventromedial	3.52 ± 0.57	4.00 ± 0.51	3.26 ± 0.26	3.36 ± 0.25	0.251	0.569	0.645
Posterior	4.72 ± 0.91	4.70 ± 0.84	4.70 ± 0.54	4.71 ± 0.42	0.965	0.982	0.859
Mammillary nu	4.04 ± 0.44	4.45 ± 0.23	3.90 ± 0.51	4.15 ± 0.44	0.857	0.759	0.589
Interpeduncular nu	7.96 ± 0.83	8.07 ± 0.51	7.32 ± 0.34	7.61 ± 0.65	0.2456	0.489	0.357
Substantia nigra	4.28 ± 0.75	5.21 ± 0.42*	4.21 ± 0.90	3.95 ± 0.69	0.008		
Pretectal area	4.77 ± 1.60	6.08 ± 0.94	4.55 ± 0.53	4.58 ± 0.47	0.124	0.053	0.105
Grey layer superior colliculus	5.77 ± 0.26	5.41 ± 0.38	4.97 ± 0.47	5.20 ± 0.38	0.086	0.006	0.661
Superior colliculus	5.57 ± 1.17	5.11 ± 0.47	4.97 ± 1.10	4.99 ± 1.00	0.558	0.382	0.581

Brain region	Vehicle		Carbamazepine (CBZ)		CBZ × Quinpirole Interaction P-value	CBZ Effect P-value	CBZ Effect P-value
	Saline (n = 5)	Quinpirole (n = 6)	Saline (n = 6)	Quinpirole (n = 6)			
Inferior colliculus	7.32 ± 0.26	7.85 ± 0.78	7.24 ± 0.30	7.51 ± 0.51	0.857	0.569	0.645
Flocculus	5.63 ± 0.33	5.89 ± 0.51	5.39 ± 0.35	5.22 ± 0.40	0.179	0.459	0.768
Cerebellar gray matter	5.03 ± 0.97	5.61 ± 1.11	5.09 ± 0.35	5.17 ± 0.79	0.493	0.645	0.368
Molecular layer cerebellar gray	7.10 ± 0.51	7.65 ± 0.51	6.52 ± 0.47	6.49 ± 1.02	0.458	0.485	0.414
White matter							
Corpus callosum	3.38 ± 0.45	3.39 ± 0.45	3.11 ± 0.46	2.95 ± 0.34	0.630	0.061	0.695
Zona incerta	3.69 ± 0.50	3.53 ± 0.32	3.47 ± 0.63	3.55 ± 0.27	0.530	0.612	0.848
Internal capsule	2.65 ± 0.25	2.84 ± 0.38	2.42 ± 0.48	2.69 ± 0.41	0.819	0.259	0.176
Cerebellar white matter	3.04 ± 0.21	2.73 ± 0.25	2.77 ± 0.56	3.03 ± 0.43	0.546	0.569	0.651
Non-blood-brain barrier regions							
Subfornical organ	5.85 ± 0.19	5.77 ± 0.34	5.49 ± 0.31	5.24 ± 0.42	0.551	0.311	0.238
Median eminence	4.53 ± 0.99	5.02 ± 0.51	4.87 ± 0.51	4.80 ± 0.74	0.347	0.489	0.845
Choroid plexus	20.9 ± 3.25	19.6 ± 2.01	19.1 ± 1.69	19.0 ± 2.03	0.477	0.333	0.480

Abbreviations: nu, nucleus; k* = (ml/s/g) × 10⁻⁴. Each k* value is a mean ± SD

Main effects are not reported if statistically significant CBZ × quinpirole interaction, when unpaired t-tests were performed.

* P < 0.05;

** P < 0.01;

*** P < 0.001; Vehicle plus quinpirole versus vehicle plus saline, CBZ plus saline versus vehicle plus saline, and CBZ plus quinpirole versus CBZ plus saline

Table 4

Effect of quinpirole on brain PGE₂ and TXB₂ concentrations in vehicle- and CBZ-treated rats

	Vehicle		CBZ		CBZ × quinpirole interaction P-value	Quinpirole effect P-value
	Saline	Quinpirole	Saline	Quinpirole		
PGE ₂ (ng/g brain)	13.8 ± 2.3	23.1 ± 4.5 *	10.4 ± 1.5 *	9.8 ± 0.6	0.003	
TXB ₂ (pg/g brain)	60.0 ± 2.6	46.3 ± 9.1	39.0 ± 8.9	33.0 ± 1.1	0.261	<0.001

Each value is a mean ± SD (*n* = 4).

* *P* < 0.05; Vehicle plus quinpirole versus vehicle plus saline, CBZ plus saline versus vehicle plus saline, and CBZ plus quinpirole versus CBZ plus saline